

Coadsorption of CO and C₆H₆ on Co(0001)

K. Habermehl-Ćwirzeń^{a,b,*}, J. Lahtinen^a, P. Hautojärvi^a

^a *Laboratory of Physics, Helsinki University of Technology, P.O. Box 1100, FIN-02150 Hut, Finland*

^b *Department of Material Science, Darmstadt University of Technology, Petersenstr. 23, D-64287 Darmstadt, Germany*

Received 22 September 2004; accepted for publication 22 December 2004

Available online 13 April 2005

Abstract

We have studied the influence of CO on the adsorption of benzene on the Co(0001) surface using LEED, XPS, TDS and work function measurements. CO was found to reduce the benzene adsorption, but even at saturation CO exposure no complete blocking was observed. Thermal desorption of the coadsorbed layer featured CO and H₂ peaks indicating partial dehydrogenation of benzene and retaining of the CO bond. Ordered LEED structures were found with all coverages: Pre-adsorption of CO led to patterns already seen for pure carbon monoxide adsorption. Pre-adsorption of benzene showed the known $(\sqrt{7} \times \sqrt{7})R19^\circ$ structure of pure benzene also with small CO exposures, but higher CO exposures yielded a mixture of $(\sqrt{7} \times \sqrt{7})R19^\circ$ and $(\sqrt{3} \times \sqrt{3})R30^\circ$ patterns.

© 2005 Elsevier B.V. All rights reserved.

Keywords: Aromatics; Carbon monoxide; Catalysis; Cobalt; Low energy electron diffraction (LEED); Low index single crystal surfaces; Thermal desorption spectroscopy; X-ray photoelectron spectroscopy

1. Introduction

Several research groups have studied the coadsorption of benzene with carbon monoxide on well-defined transition metal surfaces. Benzene serves as an ideal model for studying the adsorption and desorption of aromatic molecules. On the other hand, CO is present in almost all cata-

lytic processes, either as reactant or as contamination. Besides, CO is a perfect coadsorbate as it is both simple and well studied.

The coadsorption of benzene with carbon monoxide has been studied on Ru(0001) [1,2], Pd(111) [3,4], Pt(111) [5], Ni(100) and Ni(111) [6–9] and Rh(111) [5,10–12]. Pure benzene adsorption on Ni(111) below 270 K is reported to generate a $(\sqrt{7} \times \sqrt{7})R19^\circ$ -(C₆D₆) LEED structure, which vanishes above 300 K. Coadsorption with CO at 310 K reorders the layer to $(2\sqrt{3} \times 2\sqrt{3})R30^\circ$ -(C₆D₆ + 2CO), regardless of the sequence of exposure [7–9]. Benzene on Rh(111) is reordered by

* Corresponding author. Address: Laboratory of Physics, Helsinki University of Technology, P.O. Box 1100, FIN-02150 Hut, Finland. Fax: +358 09 451 3116.

E-mail address: kha@fyslab.hut.fi (K. Habermehl-Ćwirzeń).

CO coadsorption at 300 K. While pure benzene adsorbs in a $(2\sqrt{3} \times 3)$ structure, it changes with coadsorbed CO to $c(2\sqrt{3} \times 4)-(C_6H_6 + CO)$ and with higher CO exposures to $(3 \times 3)-(C_6H_6 + 2CO)$ [5]. The (3×3) LEED pattern is obtained independently on the sequence of exposure.

Our motivation for this study on cobalt is threefold. First, this system can be used as a model for cobalt-based catalytic processes. Benzene serves here as a model molecule for more complicated aromatic molecules.

Second, our former study of benzene adsorption on Co(0001) shows that two different adsorption structures can be found, depending on the benzene amount and on the adsorption temperature. At low exposures (<20 L) a $c(2\sqrt{3} \times 4)$ rect structure is observed. If the adsorption temperature is lower than 220 K a $(\sqrt{7} \times \sqrt{7})R19^\circ$ structure appears [13]. As CO shows a re-ordering effect on benzene on Rh(111) and Ni(111) [6–8,10–12] it raises the question whether CO coadsorption also influences the ordered structures of benzene on Co(0001).

Third, the coadsorption of CO and benzene enhances the understanding of the influence of an electron-acceptor molecule on an electron-donor molecule. Our earlier study [13] shows that pure benzene decreases the work function of Co(0001). Therefore benzene can be seen as an electron donor for cobalt, while CO is known to act as an electron acceptor. This suggests an attractive interaction between coadsorbed CO and benzene on Co(0001).

2. Experimental

The experiments included work function measurements (WF or $\Delta\Phi$), low energy electron diffraction (LEED), thermal desorption spectroscopy (TDS) and X-ray photoelectron spectroscopy (XPS). The experimental set-up has been described in detail earlier [14–16].

Our sample was a Co(0001) single crystal, with a diameter of 11 mm. This crystal was fixed to the sample holder by spot-welded tantalum wires. Additionally, these wires were used for conducting the heating current to the sample. Information on

the initial cleaning of the crystal can be found in [15,16]. This cleaning process left the sample in such a good cleanliness that a rapid cleaning by argon sputtering and annealing before each experiment was enough to obtain a clean surface. The XPS and LEED measurements before each experiment confirmed the cleanliness.

The benzene was purified by repeated freeze–pump–thaw cycles in liquid nitrogen. The exposures were measured using the uncorrected ion gauge readings. Exposure temperatures were below 200 K, which is below the desorption temperature of molecular benzene.

TDS measurements were performed with a linear temperature ramp of 2.1 K/s. Keeping the sample after TDS at the maximum temperature used during thermal desorption (~ 650 K), prevented all re-adsorption. The temperature region for conducting the measurements was restricted. Measurements were possible down to temperatures as low as 160 K. The upper temperature was limited by the non-reversible phase transition of cobalt from hcp to fcc at 690 K. The actual temperature of the sample was measured by a spot-welded thermocouple.

During XPS measurements the sample was biased at -25 V. This was done to ensure that the photoelectrons originated only from the sample and to exclude contributing signals from the sample holder or supporting structures.

3. Results and discussion

3.1. Carbon monoxide pre-adsorption

The coadsorption experiments were carried out at 180 K with CO pre-covered surfaces. CO exposures up to 8.5 L and a C_6H_6 exposure of 14 L were used.

The values for the change in the work function $\Delta\Phi$ as a function of pre-adsorbed CO are plotted in Fig. 1 before (a) and after (b) thermal desorption. The WF for the clean Co(0001) sample is set to zero on the $\Delta\Phi$ scale. The value obtained for 0 L of CO is naturally the same as for pure benzene adsorption, -1.3 eV. For CO exposures below 1 L the WF remained below the clean

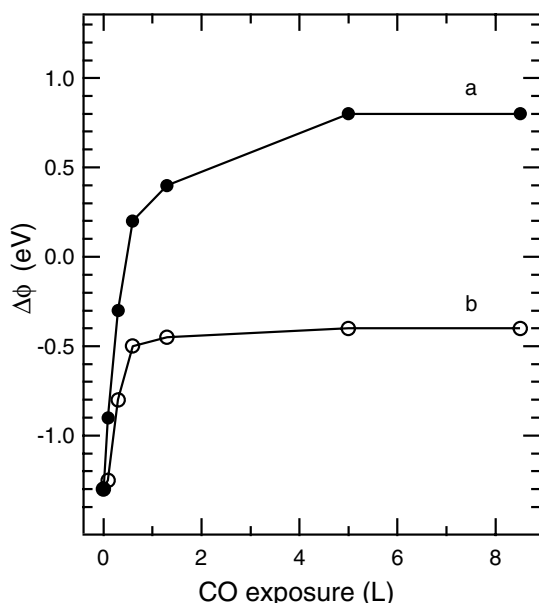


Fig. 1. Work function change $\Delta\phi$ versus CO exposure after 14 L of post-adsorbed benzene at 180 K before (a) and after (b) TDS. $\Delta\phi$ for the clean Co(0001) surface is set to be 0 eV.

surface value. Above 1 L the joint effect of CO and C_6H_6 led to an increase in the WF, which saturated at about 0.8 eV. The shape of the WF curve indicated a competing effect of CO and benzene. The WF trend as a function of increasing CO exposure was in accordance with pure CO adsorption, although the saturation value was smaller (1 eV with pure CO) [14].

The TD spectra measured after pre-adsorbed CO followed by C_6H_6 showed desorption peaks corresponding to H_2 and CO and a negligible benzene peak; no other desorption products like water, O_2 or CO_2 , were detected. The temperature maximum of the hydrogen peak was the same as in the case of pure benzene adsorption. We also found that the TDS peaks of CO were similar in position and intensity with and without benzene adsorption indicating that adsorption of benzene did not lead to an immediate desorption of pre-adsorbed carbon monoxide and all CO desorbed during heating. The CO– C_6H_6 attraction seemed to be small as the CO peaks remained at the positions obtained with pure CO adsorption.

The WF change recorded after TDS as a function of CO exposure saturated at -0.4 eV as

shown in Fig. 1. This change in the $\Delta\phi$ resulted from the remaining hydrocarbon fragments on the substrate and is therefore dependent on the amount of adsorbed benzene prior to TDS.

Pre-adsorbed CO influenced the LEED pattern as well. Up to 1 L of CO and 14 L of C_6H_6 the LEED pattern showed the $(\sqrt{7} \times \sqrt{7})R19^\circ$ symmetry seen with adsorption of pure benzene corresponding to the benzene coverage of 0.143 ML. With higher CO exposures the known [14] CO structures were successively seen: Above 1 L of CO the $(\sqrt{3} \times \sqrt{3})R30^\circ$ pattern was observed, further exposure led to the $(\sqrt{7/3} \times \sqrt{7/3})R10.9^\circ$ pattern and above 2 L of CO the $(2\sqrt{3} \times 2\sqrt{3})R30^\circ$ pattern was obtained. After TDS no LEED pattern was observable.

XPS measurements of the coadsorbed system before TDS are shown in Fig. 2. The spectra obtained for 0–3.2 L of pre-adsorbed CO with 14 L of benzene are presented. With pure benzene one peak at 285.1 eV was obtained. Adsorption of CO resulted in a second C1s peak at 286.2 eV.

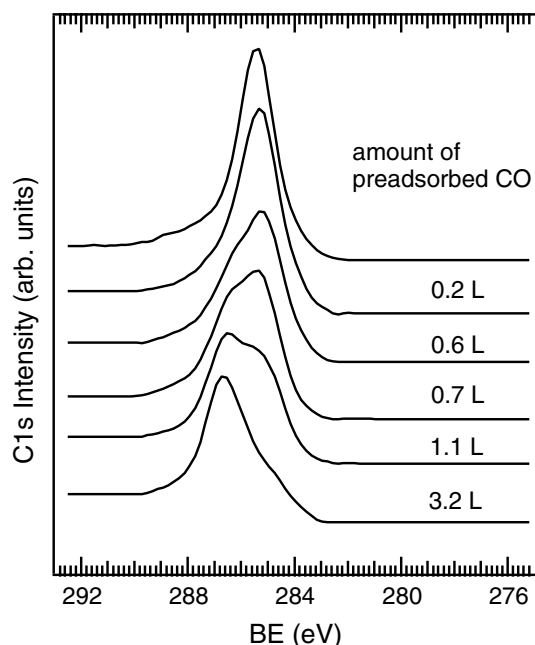


Fig. 2. Photoelectron spectra of coadsorbed CO and C_6H_6 . The spectra are arranged with increasing amount of pre-adsorbed CO from top to bottom spectrum.

Above 1.1 L of CO this C1s peak, assigned to carbon monoxide, became dominant in the spectrum. The binding energy of the CO peak stayed constant at 286.2 eV. This value corresponds to the binding energy for the on-top site in the case of pure CO adsorption [14,17]. The binding energy of the benzene peak decreased steadily with increasing amount of pre-adsorbed CO from 285.1 eV for 0 L of CO to 284.5 eV for 6 L of CO. Since benzene adsorbs flat at an hcp site in the $\text{Co}(0001)-(\sqrt{7} \times \sqrt{7})R19^\circ\text{-C}_6\text{H}_6$ structure [18], we expect the benzene molecules to remain at these sites at low CO exposures. Since there are empty on-top sites in the $(\sqrt{7} \times \sqrt{7})R19^\circ\text{-C}_6\text{H}_6$ structure available, and the C1s binding energy for the CO peak indicates adsorption at the top sites, we suggest this site for CO in the presence of benzene (Fig. 3). This is supported by the adsorption structures obtained on other transition metals, where similar adsorption sites are observed for both CO and C_6H_6 [3–5,11,12]. When the CO coverage exceeded that of C_6H_6 , the CO molecules at the on-top sites started to dominate and the adlayer exhibited the $(\sqrt{3} \times \sqrt{3})R30^\circ$ symmetry. At

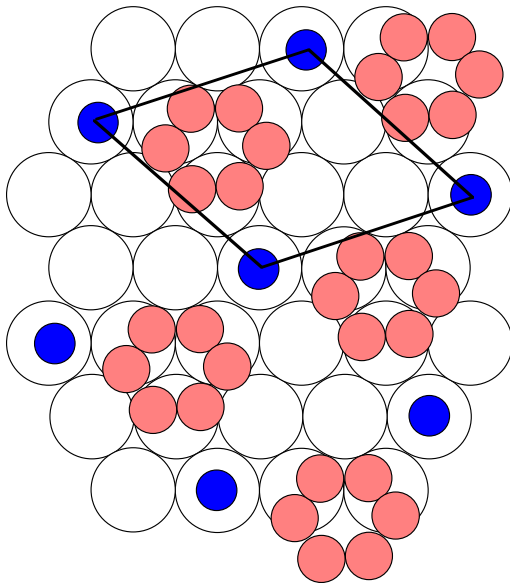


Fig. 3. Proposed $(\sqrt{7} \times \sqrt{7})R19^\circ\text{-C}_6\text{H}_6 + \text{CO}$ coadsorption structure on $\text{Co}(0001)$. The adsorption sites are based on the adsorption on pure CO and pure benzene on $\text{Co}(0001)$.

this stage we assume that the benzene molecules were displaced from the hcp sites and could even have changed their orientation.

The XPS intensities after coadsorption indicate that the area of the CO peak clearly increased with increasing CO exposure as long as the saturation level was not reached. At the same time the C1s peak originating from post-adsorbed benzene seemed to decrease drastically. Fig. 4 illustrates this by showing the peak areas after 14 L of benzene and 0–8.5 L of pre-adsorbed CO. It is evident that the pre-adsorbed CO stayed on the surface during benzene adsorption. As the CO coverage increased to saturation, the value for benzene saturation dropped to 1/3 compared to the value for pure benzene adsorption. XPS spectra were also taken after TDS. The binding energies of the carbon atoms left on the surface after heating—the so-called benzene fragments—did not change with CO pre-coverage; being 285.7 eV and 284.4 eV. Adding up the peak areas obtained for the benzene fragments, we noticed that the total amount of

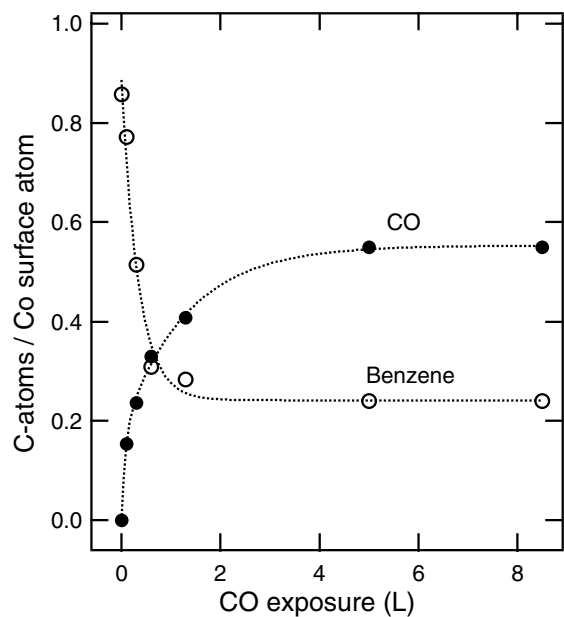


Fig. 4. Carbon atom coverage versus CO exposure. The benzene exposure was 14 L. The solid markers correspond to CO and the open markers to C_6H_6 data. All lines are drawn to guide the eye.

carbon on the surface decreased to 30% compared to single benzene adsorption. We can thus conclude that there was partial site blocking for benzene due to CO pre-adsorption.

3.2. Benzene pre-adsorption

We repeated the adsorption measurement by reversing the order of adsorption. In this case the benzene exposure was 14 L and CO exposures varied between 0 L and 66 L.

For pure benzene adsorption on Co(0001), TDS revealed H₂, originating from dissociated C₆H₆, and a negligible amount of C₆H₆ as desorption products [13]. Pure carbon monoxide is known to desorb during heating as an intact molecule from the Co(0001) surface [14]. The TDS spectra measured after 14 L of C₆H₆ followed by different amounts of CO are shown in Fig. 5.

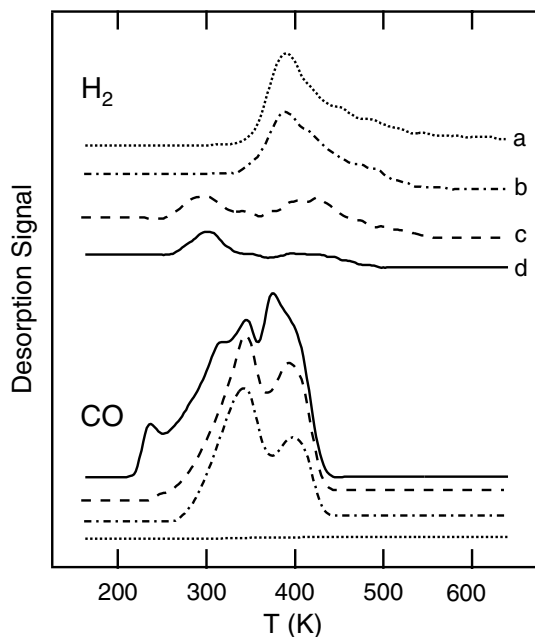


Fig. 5. Thermal desorption spectra obtained after pre-adsorption of benzene along with adsorbed carbon monoxide. The adsorption took place below 180 K and the heating rate was 2.1 K/s. Hydrogen and CO spectra are shown but benzene spectra are not included as benzene desorption is in all cases negligible. The letters indicate different exposures: pure benzene (a), benzene and 5 L of CO (b), 16 L of CO (c), 66 L of CO (d).

Major desorption peaks were only detected corresponding to H₂ and CO; no new desorption products were detected and benzene desorption upon heating was negligible.

The adsorption of CO influenced the dehydrogenation of benzene on the Co(0001) surface, as it is reflected in the TDS results of Fig. 5: Spectra (a) were obtained for pure benzene adsorption. Spectra (b) obtained after 5 L of CO and show a 25% decrease in the hydrogen signal. Further increase in CO exposure resulted in further decrease in the hydrogen signal as well as a splitting of the signal into a high temperature and low temperature peak (c). Even higher exposures of CO were followed by the diminishing of the high temperature peak (d). For an exposure of 66 L of CO the hydrogen signal had decreased to about 30% compared to the signal for pure benzene adsorption.

This change in the hydrogen signal was found for CO post-adsorption as well as CO pre-adsorption. Its origin was in the latter case the blocking of benzene adsorption. For CO post-adsorption the reduction is explained by pronounced displacement of benzene from the surface.

When benzene was pre-adsorbed, the work function changes were different to the previous case. In accordance with [13] $\Delta\Phi$ of -1.3 eV compared to the clean surface was reached after saturation exposure of benzene. Below 3 L of post-adsorbed CO no change in the work function was recorded. Above 3 L $\Delta\Phi$ started to increase due to CO adsorption but large exposures were needed to obtain values $\Delta\Phi > 0$. The curve saturates around 66 L of CO at $+0.8$ eV, having the same saturation value as with CO pre-adsorption.

The more than 10 times higher CO exposure needed had its origin both in site blocking and electrostatic effects. The benzene molecules blocked the adsorption of CO on the surface and thus the effective sticking was decreased. This is evident based on the gentle slope of the WF change curve at small CO exposures (not shown). After some CO was adsorbed within the benzene layer the mutual interactions started to favour CO adsorption but the sticking remained still lower than in the case of CO only.

Changes in the C1s peak area were similar to the case of CO pre-adsorption, except for the CO

exposure scale. As before, the peak area of the benzene peak decreased to one third for 66 L of coadsorbed CO. Simultaneously the area of the CO peak increased as in the case of benzene post-adsorption.

After TDS, the C1s peaks were alike as with CO pre-adsorption. Although it took larger CO exposures in the case of CO post-adsorption, the adsorption sequence itself had no influence on the amount of hydrocarbon fragments obtained after thermal desorption.

The $\Delta\Phi$ change measured after TDS for 14 L of C_6H_6 was -0.4 eV. This value is identical to the value obtained with pre-adsorbed CO indicating total desorption of CO and formation of the same hydrocarbon fragments on the surface independent on the adsorption order.

For the pre-adsorption of benzene three different LEED structures were distinguished: Exposing the surface to benzene gave rise to the $(\sqrt{7} \times \sqrt{7})R19^\circ$ - C_6H_6 structure, which remained on the surface during the initial stages of CO adsorption. Above 5 L of CO new spots featuring the

$(\sqrt{3} \times \sqrt{3})R30^\circ$ symmetry appeared in addition to the original benzene structure (Fig. 6). The presence of simultaneous LEED spots was assigned to island formation for both species on the surface. Within these islands the adsorbates reside at their optimal adsorption sites. Earlier such a superposition of two LEED structures has been found for NO and C_6H_6 coadsorption on Ni(111) [9]. With more than 15 L of CO, the LEED pictures revealed a $(2\sqrt{3} \times 2\sqrt{3})R30^\circ$ structure, which is known for high exposures of pure CO at 200 K on clean Co(0001) [14]. This is again similar to the case of pre-adsorbed CO. After TDS no ordered LEED structure was found.

Taking the XPS data into account, we claim that the LEED structures were influenced by the partial desorption of benzene enabling the CO–CO interaction to overcome the C_6H_6 – C_6H_6 interaction. This difference in the interaction strength for these molecules was suggested earlier by Mate and Somorjai [5].

4. Conclusions

The coadsorption of benzene and carbon monoxide on Co(0001) was studied by LEED, XPS, TDS and work function measurements. The results are mainly independent on the adsorption order of the coadsorbates.

During thermal desorption hydrogen, CO and a negligible amount of benzene are released, but desorption of other hydrocarbons, like acetylene or biphenyl, is not detected. The amount of desorbed hydrogen decreases as the CO exposure is increased. The reduction in the hydrogen desorption results from site blocking/induced desorption of C_6H_6 caused by CO. However complete quenching is not observed. The data also suggest that the CO–benzene attraction remains small.

LEED results depend on the sequence of adsorption. For small amounts of pre-adsorbed CO the LEED pattern features the pure benzene structure. With CO exposures higher than 1 L the pattern changes successively to those observed without benzene adsorption. In the case of pre-adsorbed benzene, again the $(\sqrt{7} \times \sqrt{7})R19^\circ$ benzene-only structure appears in the beginning.

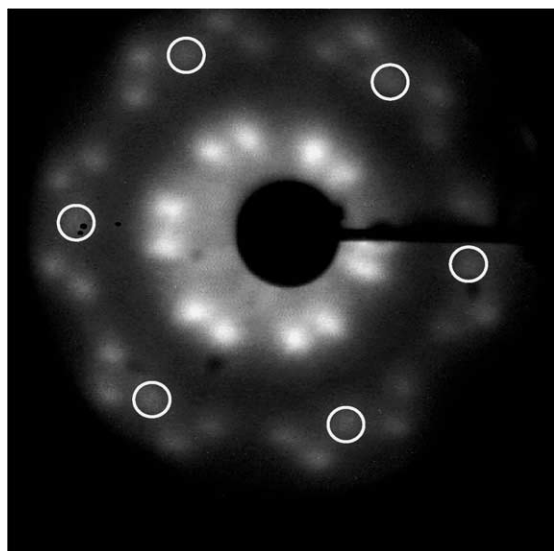


Fig. 6. LEED pattern after 14 L of benzene followed by 5 L of CO on Co(0001). The pattern is a combination of $(\sqrt{7} \times \sqrt{7})R19^\circ$ from C_6H_6 and $(\sqrt{3} \times \sqrt{3})R30^\circ$ from CO. The spots featuring the $(\sqrt{3} \times \sqrt{3})R30^\circ$ pattern are marked with white circles.

With higher CO exposures we were able to see simultaneously the $(\sqrt{3} \times \sqrt{3})R30^\circ$ pattern indicating island formation of the adsorbates. With increased CO exposure these two structures disappear and the $(2\sqrt{3} \times 2\sqrt{3})R30^\circ$ structure, known for pure CO exposure, is seen. This general trend towards structures seen with pure CO is due to the stronger mutual interaction between CO molecules compared to C_6H_6 molecules.

In both cases CO adsorbs only at on-top sites, independent of the amount of adsorbed CO. The benzene molecules are adsorbed flat on the surface at threefold hollow sites except with high CO coverage where the adsorption site or the orientation of the benzene molecule is believed to change.

After the thermal desorption two carbon peaks originating from benzene fragments at 284.4 eV and 285.7 eV are obtained in both cases. These peaks are also found with pure benzene adsorption [13]. This finding is in line with TPD results in [6] where CO on Ni(100) reduces the desorption of benzene but does not induce a complete depletion of adsorbed benzene.

Work function measurements show that CO increases the $\Delta\Phi$, whereas benzene decreases it. In both adsorption cases a considerable amount of CO leads to the $\Delta\Phi$ saturation value of 0.8 eV. The saturation value for $\Delta\Phi$ after TDS is approximately -0.4 eV.

In conclusion, CO adsorption is blocking the benzene adsorption by a factor of 3 on the surface. This is true for both pre-adsorbed CO, where blocking of benzene adsorption is detected, and post-adsorbed CO, where benzene desorption is induced. In both cases, however, some benzene is still left on the surface even at saturation CO exposures.

Acknowledgement

We thank the Academy of Finland and the National Graduate School in Materials Physics for supporting this research.

References

- [1] P. Jakob, D. Menzel, Surf. Sci. 235 (1990) 15.
- [2] P.A. Heimann, P. Jakob, T. Pache, H.-P. Steinrück, D. Menzel, Surf. Sci. 210 (1989) 282.
- [3] H. Ohtani, M.A. Van Hove, G.A. Somorjai, J. Phys. Chem. 92 (1988) 3974.
- [4] H. Ohtani, B.E. Bent, C.M. Mate, M.A. Van Hove, G.A. Somorjai, Appl. Surf. Sci. 33/34 (1988) 254.
- [5] C.M. Mate, G.A. Somorjai, Surf. Sci. 160 (1985) 542.
- [6] P.M. Blass, S. Akhter, J.M. White, Surf. Sci. 191 (1987) 406.
- [7] H.-P. Steinrueck, W. Huber, T. Pache, D. Menzel, Surf. Sci. 218 (1989) 293.
- [8] W. Huber, P. Zebisch, T. Bornemann, H.-P. Steinrueck, Surf. Sci. 258 (1991) 16, and references within.
- [9] W. Huber, H.-P. Steinrueck, T. Pache, D. Menzel, Surf. Sci. 217 (1989) 103.
- [10] E. Bertel, G. Rosina, F.P. Netzer, Surf. Sci. 172 (1986) L515.
- [11] M.A. Van Hove, R.F. Lin, G.A. Somorjai, J. Am. Chem. Soc. 108 (1986) 2532.
- [12] R.F. Lin, G.S. Blackman, M.A. Van Hove, G.A. Somorjai, Acta Cryst. B 43 (1987) 368.
- [13] K. Habermehl-Cwirzen, J. Katainen, J. Lahtinen, P. Hautojärvi, Surf. Sci. 507–510 (2002) 57.
- [14] J. Lahtinen, J. Vaari, K. Kauraala, Surf. Sci. 418 (1998) 502.
- [15] J. Lahtinen, J. Vaari, A. Talo, A. Vehanen, P. Hautojärvi, Surf. Sci. 245 (1991) 244.
- [16] J. Lahtinen, J. Vaari, A. Talo, A. Vehanen, P. Hautojärvi, Vacuum 41 (1990) 112.
- [17] J. Lahtinen, J. Vaari, K. Kauraala, E.A. Soares, M.A. Van Hove, Surf. Sci. 448 (2000) 269.
- [18] K. Pussi, M. Lindroos, J. Katainen, K. Habermehl-Cwirzen, J. Lahtinen, A tensor LEED determination of the structure of $Co\{0001\}-(\sqrt{7} \times \sqrt{7})R19.1^\circ-C_6H_6$, Surf. Sci. 572 (2004) 1.